Polytechnic University of Turin

DEPARTMENT OF ENERGY

Master of Science degree in Mechanical Engineering

3-D CFD simulations of a dual fuel two-stroke marine engine

Lean combustion analysis for Diesel ignited NG

Thesis advisors:

Prof. Dr. Ezio Spessa

Prof. Dr. Konstantinos Boulouchos

Research supervisor:

Dr. Michele Bolla

Candidate:

Antonio Totaro

Academic year 2017/2018

Abstract

During the following Master thesis work the switching of a diesel 2-stroke marine engine into a dual fuel one was assessed. As the project was carried on at LAV (Labor für Aerothermochemie und Verbrennungssysteme), at ETH Zürich, in collaboration with the Winterthur Gas & Diesel AG company, we were required to focus our analytical study above all on the combustion process of one of the RTX-5 engine cylinders: by applying a LES (Large Eddy Simulation) approach, we took advantage of the FGM (Flamelet Generated Manifold) combustion model and went on making a comparison between the results obtained by means of the above mentioned model, which was used at LAV, with the one taken into account by the Winterthur Gas & Diesel AG company, the PV (Progress Variable) model.

Acknowledgements

I would like to thank Prof. Ezio Spessa, Prof. Konstantinos Boulouchos and Dr. Michele Bolla for offering me the opportunity to write my Master's thesis at ETH Zurich under their supervision. Without their guidance this work would not have been possible.

I owe my deepest gratitude to Dr. Michele Bolla for his patience, professionalism and seriousness and for providing me with crucial information and aids.

I would also like to thank, from the heart, my family which have always been an immeasurable support for my studies and my personal growth, the warm-hearted Giuppini family and all the funny guys I met at camp Axa in Winterthur during the 6 months of work on this project.

Contents

List of Figures **VIII**

List of Tables **X**

Introduction **1**
Cylinder features 6
Initial and boundary conditions 12

Methodology **14**
Flamelet Generated Manifold 14
Implementation of FGM 15
Computational set-up 24

Results and discussion **28**
Control parameter: Progress Variable variance 28
Control parameter: Csource ignition term 33
Control parameter: methane mixture fraction 36

Conclusion **38**

Bibliography **42**

List of Figures

1 Conceptual model of quasi-steady diesel combustion plume as presented by Prof. J. Dec (1999) [6]. 2
2 Premixed combustion. 3
3 The visualization of 3D tumble flow: (left) geometric visualization using streamlines, (middle-left) geometric visualization streamlines accompanied by texture-based flow visualization on a 2D slice, (middle-right) geometric flow visualization using timelines, combined with texture-based flow visualization on a velocity isosurface, and (right) geometric flow visualization with streamlines and a pressure isosurface color-mapped with velocity magnitude [7]. 4
4 The visualization of swirl flow in the volume of the the combustion chamber: (left) direct visualization using color-mapped glyphs, (middle-left) geometric flow visualization using color-mapped shaded streamlines, (middle-right) texture-based flow visualization on a velocity isosurface, and (right) isosurfacing combined with 3D streamlines [7]. 5
5 Dual fuel RTX-5 engine geometry. 6
6 +z axis view. 7
7 On the left hand side is the +y axis view. On the right the +x axis view. 7
8 IMEP cyclic variation and experimental pressure trace. 9
9 OH photomultiplier signals with different λ_{CH_4} with the injection profile a specified injector [16]. 11
10 Schematic illustration of an experimental configuration for counterflow diffusion flames [11]. 19
11 Scalars initialization in Pro-Star (1). 21
12 Scalars initialization in Pro-Star (2). 22
13 Scalars initialization in Pro-Star (3). 23
14 In-cylinder mass trend for the non-reactive phase. 25
15 Computed (blue line) and experimental (red line) IMEP. . . . 26

16 In-cylinder IMEP and cyclic variation. 28
17 Positive pre-chamber IMEP. 29
18 In-cylinder Progress Variable. 30
19 Premixed combustion process delay between three different cylinder regions. 31
20 From top to bottom: *PVvar=0.97*, *PVvar=0.98*, *PVvar=0.99*. 32
21 Jets evolution: temperature inside the cylinder during the premixed combustion process. 33
22 Positive pre-chamber IMEP. 34
23 In-cylinder IMEP and cyclic variation. 34
24 Premixed combustion delay due to the *Csource* term. 35
25 In-cylinder Progress Variable. 35
26 In-cylinder IMEP and cyclic variation. 36
27 In-cylinder Progress Variable. 37

List of Tables

1 RTX-5 operating condition. 10
2 RTX-5 initial and BCs. 13

Introduction

Two of the main objectives in improving our limited understanding of the combustion processes in engineering applications is to enhance the efficiency of conventional systems and to find effective means to curb the problem of air pollution coping with the more and more strict emission standards, the legal requirements governing air pollutants released into the atmosphere. Moreover, the rapid depletion of conventional fuel resources has focused attention towards developing economically a relatively clean and efficient burning alternate fuel. Attention is being focused on various gaseous fuels, and in particular natural gas (NG).

Among the alternative fuels, methane (CH4), the main element in the natural gas mixture, is considered very promising both because it can work with high compression ratios without experiencing the knock phenomenon and because of lower fuel and maintenance costs, longer engine life and its increased availability. Most combustion devices are adaptable relatively easily to the use of natural gas for power production. Particularly, high compression ratio piston engines (i.e. diesel engines) are generally suitable when high thermal efficiency is desired. However, it is necessary to prime the combustion. This can be obtained either using a spark plug, similar to what happens in gasoline engines or spraying a certain quantity of diesel fuel, whose ignition and combustion sets the combustion of methane.

From this perspective, the Winthertur Gas & Diesel AG company aims to design and manufacture a new model of marine engine by renewing an old diesel ship propelling system just turning it into a dual fuel one, which combines the low combustion reactivity of the natural gas, mostly methane, with the high combustion reactivity of the n-dodecane ($C_{12}H_{26}$) which works as trigger for the whole blend.

The dual fuel combustion system features essentially a homogeneous gas-air blend compressed rapidly below its autoignition conditions, and ignited

by the injection of pilot liquid fuel near the top dead center position. The primary fuel is generally gaseous at atmospheric conditions and controls the power output. The pilot liquid fuel, which is injected through the conventional diesel injectors, normally contributes only a small fraction of the maximum power output. Hence the overall turbulent combustion process takes place in two phases:

- non-premixed phase
- premixed phase

In the first phase, the evolution of the combustion process of the small amounts of diesel pilot injections is investigated. Diffusive flames are generated by the combination of oxidizer (air + methane) and n-dodecane for high p and T in-cylinder conditions. The combustion process takes place at the flames' surface only, where the diesel fuel meets oxygen in the right concentration (equivalence ratio, $\phi \sim 1$): while the interior of the flames, in which the equivalence ratio is greater than the stoichiometric, contains unburnt fuel, unburned hydrocarbons (UHCs) like paraffins and olefins, CO and SOOT precursors (Polycyclic Aromatic Hydrocarbons, PAHs), the shell of the diesel plume, due to its higher temperatures and stoichiometric concentration, is rich of NO_x and HC.

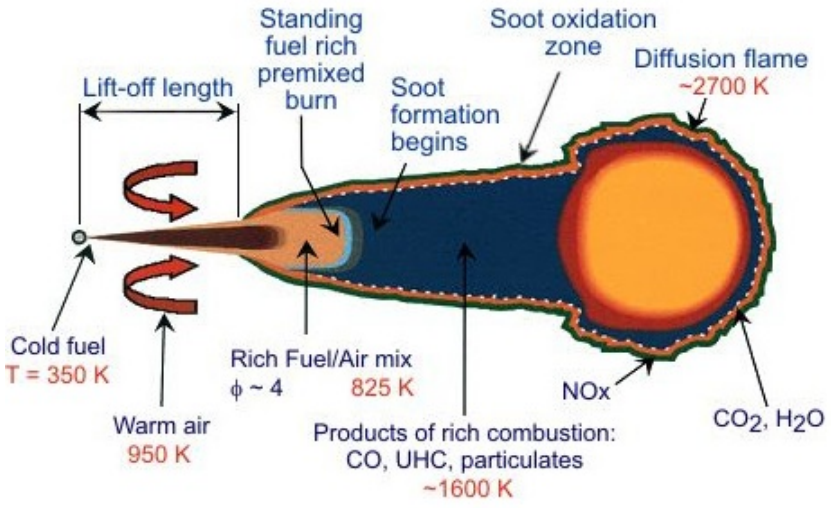

Figure 1: Conceptual model of quasi-steady diesel combustion plume as presented by Prof. J. Dec (1999) [6].

In spite of this, for the dual fuel marine engine investigated in this report the non-premixed phase concerns only tiny amount of diesel if compared either to the mass flow rate of the main fuel (methane) or to the diesel engine considered as "basic design" to be improved. Therefore all the final products of the diesel combustion process, which was analyzed by Prof. J. Dec [6], as well as every kind of combustion intermediate product, is drastically gone down reaching low concentrations at the exhaust.

The ignition of diesel pilots starts the second phase. From the first kernels of methane ignited by the diesel combustion, the premixed combustion then spreads throughout the mixture: layer after layer the flame front travels through the chamber, mainly thanks to a convective heat exchange between burned gases and the unburned mixture which is contained in the layer next to the flame front, until the last zones (also called “end gas”) more far from the first kernels are reached. The flame front speed is greatly increased by the turbulence inside the mixture (the turbulence corrugates the flame front, thus increasing the heat exchange area, and so the flame propagation speed): since turbulence intensity increases with engine revolution speed, and the flame front speed is proportional to turbulence intensity, the flame front will increase with engine speed, thus compensating the reduction of time available for combustion.

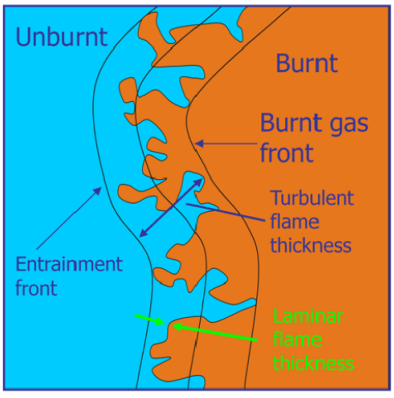

(a) Turbulent flame front propagation.

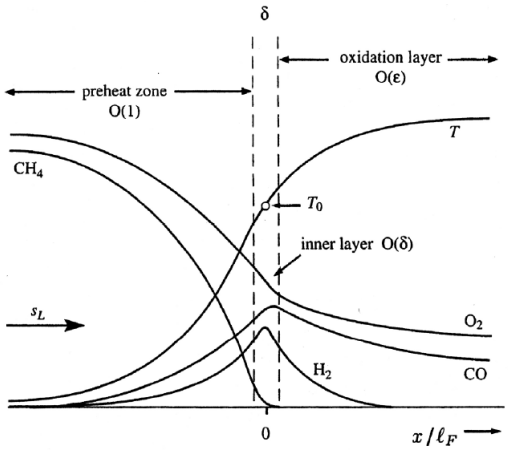

(b) Laminar flame front for methane-air stoichiometric mixture at 1 atm. S_L, laminar burning velocity. L_F, laminar flame front thickness.

Figure 2: Premixed combustion.

Actually few options are available for increasing the turbulence in the

combustion chamber and consequently speeding up the combustion process:

by enhancing tumble, an organized vortex around an axis that is perpendicular to the cylinder one (see Figure 3). Tumble is generated during expansion and, provided that it is strong enough, it is 'accelerated' during the first part of the compression stroke. Tumble is then destroyed near TDC, and converted into turbulence energy at small scales;

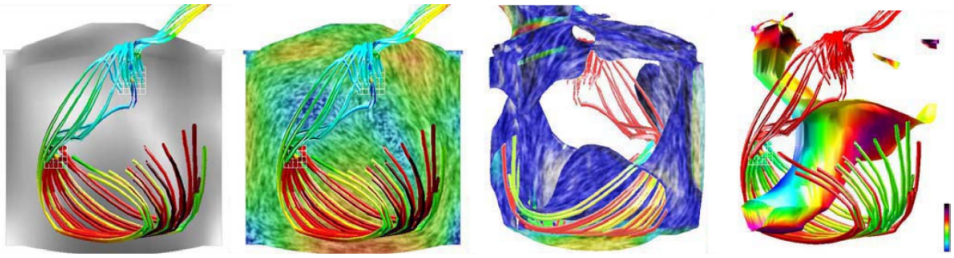

Figure 3: The visualization of 3D tumble flow: (left) geometric visualization using streamlines, (middle-left) geometric visualization streamlines accompanied by texture-based flow visualization on a 2D slice, (middle-right) geometric flow visualization using timelines, combined with texture-based flow visualization on a velocity isosurface, and (right) geometric flow visualization with streamlines and a pressure isosurface color-mapped with velocity magnitude [7].

by a suitable bowl-shape piston head which allows the squish motion, a radially-inward gas motion that occurs towards the end of the compression stroke (TDC), when a portion of the piston face and cylinder head approach each other closely. Reverse squish occurs during expansion;

by a swirl motion vortex, an organized rotation of the charge about the cylinder axis (see Figure 4). Swirl is created during the induction stroke, by bringing the intake flow into the cylinder with an initial angular momentum, for instance by means of 'directed ducts'. While some decay in swirl due to friction occurs during engine cycle, intake generated swirl usually persists through the compression, combustion, and expansion processes. In engine designs with bowl-in-piston combustion chambers, the rotational motion set up during intake is substantially modified during compression. Swirl is used in diesels and some stratified-charge engine concepts to promote more rapid mixing between the inducted air charge and the injected fuel. Swirl is also used to improve scavenging in 2-stroke engines. In the following study a swirl motion is supplied to fresh air charge and methane injections, still by means

of tangentially directed ducts towards the cylinder wall.

Figure 4: The visualization of swirl flow in the volume of the the combustion chamber: (left) direct visualization using color-mapped glyphs, (middle-left) geometric flow visualization using color-mapped shaded streamlines, (middle-right) texture-based flow visualization on a velocity isosurface, and (right) isosurfacing combined with 3D streamlines [7].

The whole engine cycle is investigated using the Large Eddy Simulation (LES) which quantifies the smallest turbulence scales by means of a closure empirical method with 2 equation models ($k - \epsilon$). On the other hand, to account for the complex chemical kinetics of reactions of combustion, Flamelet Generated Manifold (FGM) model is taken into account. The flamelet database is generated by POLIMI mechanism with a reduced number of species and reactions to be solved for the combustion process, so as to reduce the computational cost of the simulation. The Flamelet Generated Manifold approach is based on the assumption that a high-dimensional state space of chemical species can be approximated by a low-dimensional manifold (LDM) [24]. In the FGM method an LDM is obtained from a set of one-dimensional laminar flame (i.e. flamelet) calculations. Further insights about the FGM approach will be explained exhaustively in the chapter Methodology.

Cylinder features

In the following section a wide overview of the improved marine engine features is given. Winterthur Gas & Diesel AG company provided us with the main geometrical characteristics of the dual fuel engine, RTX-5, and its operating condition, on which we were required to simulate the engine cycle.

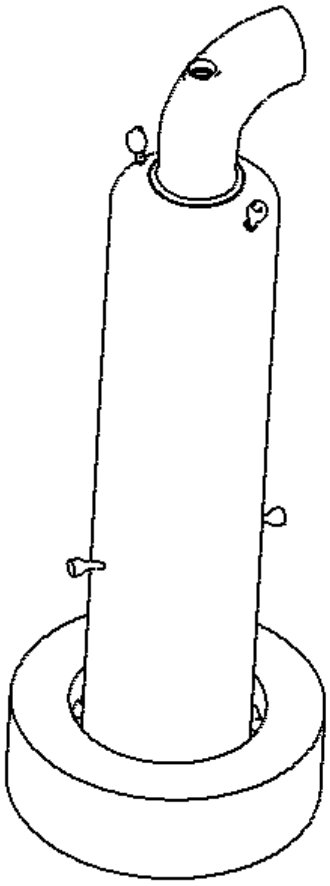

Figure 5: Dual fuel RTX-5 engine geometry.

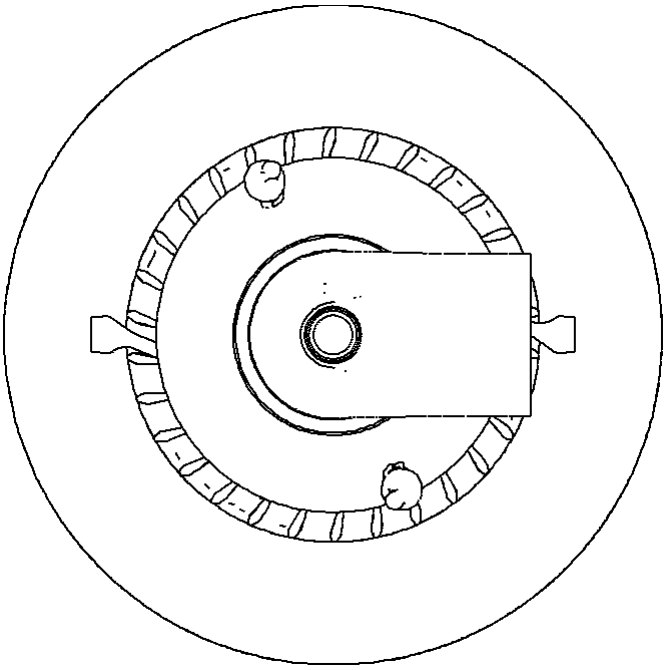

Figure 6: +z axis view.

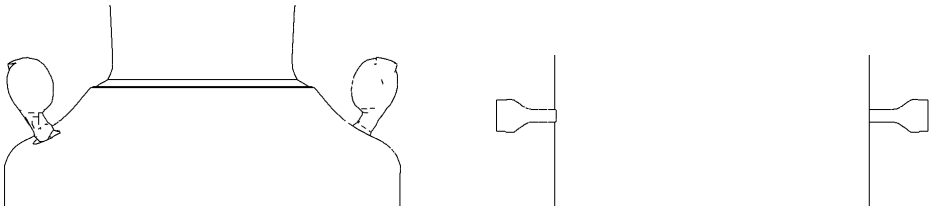

(a) Pre-chambers view on the cylinder head.

(b) GAVs, methane injectors view.

Figure 7: On the left hand side is the +y axis view. On the right the +x axis view.

As one notices in Figure 6, in the view from the top of the cylinder, and as we remembered previously, the swirl motion is supplied to fresh air charge, methane injections as well as flame jets coming out the pre-chambers by means of tangentially directed ducts towards the cylinder wall. The toroid on the bottom of the cylinder represents the intake chamber through which the fresh air gets into the cylinder main chamber crossing some tangentially directed pipes.

As for the operating condition, in the table below the basic information useful to run the simulation is summed up. Given the measured pressure traces inside the cylinder for approximately 600 engine cycles (Figure 8), a strong cyclic variation can be noticed by a remarkable difference of about 30 bar just looking at the lowest and highest pressure peak. Therefore an average IMEP (Indicated Mean Effective Pressure) is chosen as representative of the in-cylinder pressure trend. I just point out that the problem of cyclic variation, a variation in the IMEP from cycle to cycle, is more severe in two-stroke engines because of the unsteady nature of fluid flow and the higher torque fluctuations. By eliminating this cyclic variation, the engine power output can be considerably increased, moreover, the cyclic variation results in poor drivability. It is also identified that reducing the cyclic variation may suppress engine noises and vibrations.

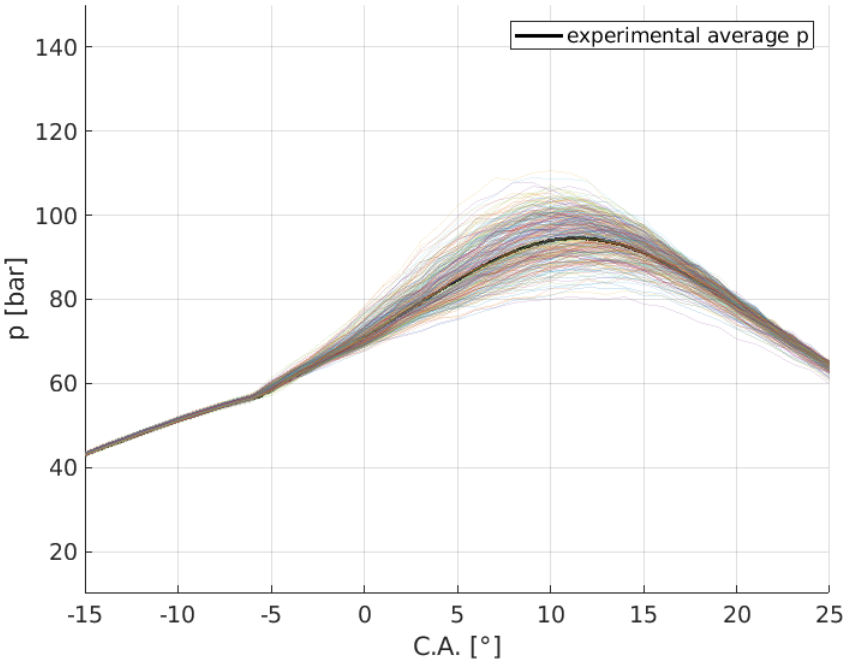

Figure 8: IMEP cyclic variation and experimental pressure trace.

RTX-5 engine non-pre-igniting operating condition	
Bore	$500\,mm$
Stroke	$2050\,mm$
Power	$4295.24\,kW$
Speed	$98.98\,rpm$
n° of cylinders	6
n° of GAVs per cyl.	2
n° of pre-chambers per cyl.	2
n° of n-dodecane injectors per prech.	1
n° of holes per injectors	3
EVO actual	$-241.40\,°CAaTDC$
EVC actual	$-119.95\,°CAaTDC$
GAV timing	$-149.05\,°CAaTDC$
GAV closure	$-131.11\,°CAaTDC$
Pilot timing	$-7.1150\,°CAaTDC$
Pilot duration	$1.1\,ms$
bsfc methane	$160.95\,g/kWh$
bsfc n-dodecane	$1.9180\,g/kWh$
bsac (air consumption)	$7.8505\,kg/kWh$
λ_{CH_4}	$2 \div 3$

Table 1: RTX-5 operating condition.

Looking at the operating condition table above, the case without pre-ignition of the methane is chosen and furthermore the combustion process happens in an environment with a lean methane-air blend ($\lambda_{CH_4} > 1$). As it is true that a lean methane combustion is a technique that results in the reduction of both pollutants NO and soot and contributes to the reduction of carbon dioxide emissions due to the low C/H ratio [10], likewise it results in various effects over the combustion process.

During the experimental study led by Prof. Dr. Konstantinos Boulouchos at ETH Zurich over the combustion characteristics of a diesel pilot spray in a lean premixed methane-air charge using a Rapid Compression Expansion Machine (RCEM), it was seen that higher values of the equivalence ratio ($\phi = 1/\lambda$) promote propagation of the premixed flame as expected, but delay the auto-ignition of the pilot spray considerably (ranging between 1.05 ms (diesel in air) and 2.28 ms ($\lambda_{CH_4} = 1.5$) [16]): filtered photomultiplier signals of the total emitted light for OH, CH and C2 radicals as well as the effect of methane content on diesel ignition locations, ignition timing and combustion behaviour was analysed.

For all the OH, CH and C2 photomultiplier signals acquired a longer signal was observed with increasing methane content which is an indication for longer combustion durations. Thus an increasing intensity of the combustion with an increasing methane amount and longer diesel ignition delay for increasing amounts of methane in the system (e.g Figure 9). With the longer ignition delay there is also more time for the pilot spray to evaporate and mix with the surrounding gas. The latter could lead to a lean premixed ignition and combustion of the pilot spray which is both slower and less intense than ignition and combustion in stoichiometric n-dodecane regions. In non-premixed situations, ignition takes place at the most reactive mixture fraction which is normally quite rich.

Nonetheless in the following study we will not get further insights about this effect but it is just to point out once again that the redesigning process of the old diesel marine engine in a dual fuel propelling system implies a number of complications to consider.

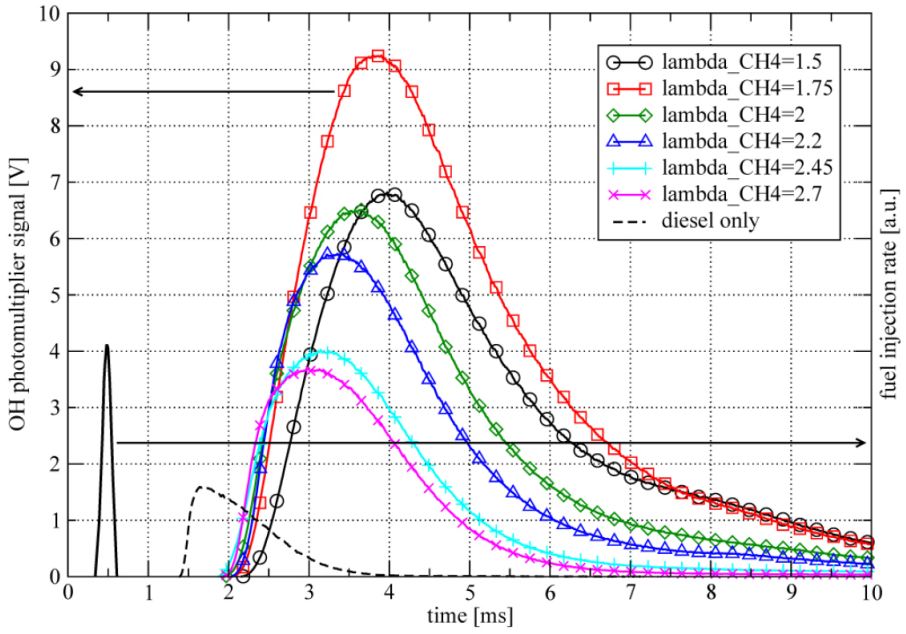

Figure 9: OH photomultiplier signals with different λ_{CH_4} with the injection profile a specified injector [16].

Initial and boundary conditions

I mention the initial and boundary conditions information retrieved from Winterthur Gas & Diesel AG company right in this section instead of describe it in the next chapter over the methodological approach pursued as I think being more in line with the steps followed before running the engine cycle simulation, namely checking and analysing the geometrical features and operating condition parameters and then moving on running the simulation.

We used two SIEMENS CFD tools, *es-ice* and *Star-CD/Pro-Star*, to create the events of the moving mesh, to initialize and set the BCs, and in the end to post-process the data obtained from the LES.

In the table 2 below, the $Scalars$ variables represents the concentrations of the species indicated, Z the mixture fraction of the methane, PV is the progress variable of the whole combustion process. As for the last two variables, the next chapter about the methodological approach adopted will give more information over the primary importance they have in the employment of the FGM combustion model. The last remark is that the GAVs are initialized in accordance to the crank angle initial position: in this case, at $-260\,°CAaTDC$ of combustion, the GAVs are looking on the volume beneath the piston, that is why the p and T are the same of the ones in the fresh air intakes. In another case, for instance with the piston position just below the GAVs' intakes, we would have to set, as p and T, the same values they get in the main chamber.

Initial and boundary conditions (at -260 °CAaTDC of combustion)		
Fresh charge intakes:	BC	INLET
	p	2.569 bar
	T	45.66 $°C$
	$Scalar_{N_2}$	0.767
	$Scalar_{O_2}$	0.233
	Z_{CH_4}	0
	PV	0
GAVs:	BC	INLET
	T	300 K
	$Scalar_{CH_4}$	1
	Z_{CH_4}	1
	PV	0
Exhaust pipe:	BC	EXHAUST
	p	2.479 bar
	T	611 K
	PV	1
Walls:	BCs	WALL
	$T_{piston\,head}$	550 K
	T_{dome}	500 K
	T_{wall}	450 K
Initialisation:	Main chamber:	
	p	7.485 bar
	T	618.5 $°C$
	Piston underside and GAVs:	
	p	2.569 bar
	T	45.66 $°C$

Table 2: RTX-5 initial and BCs.

Methodology

This chapter discusses the methodology used in this thesis to create the Flamelet Generated Manifold (FGM) tables which then served as look-up tables for Computational Fluid Dynamics (CFD) to simulate the dual fuel combustion process. Insights to the working principles and governing equations of the process are given. All the equations presented in this chapter are documented in detail in the bibliography cited from time to time.

Flamelet Generated Manifold

The Flamelet Generated Manifold (FGM) technique, which was developed at Eindhoven University of Technology by van Oijen and de Goey [9], is based on the flamelet approach which reduces the equations to be solved and thus cutting down the CPU time.

Reduction methods for chemical kinetics are based on the observation that a typical combustion system contains many chemical processes with a much smaller time scale than the flow time scales. That means that the concept is valid for high Damköhler numbers with

$$Da = \frac{\tau_t}{\tau_c} \tag{1}$$

where τ_t and τ_c are the flow and the chemical time scales, respectively. These fast chemical processes may be decoupled and assumed to be in steady state. A kinetic model is used for the chemical mechanism of the reactions of combustion and the influence of turbulence is treated with an appropriate closure method. The so called Flamelet Generated Manifold shares the idea that a turbulent flame can be seen as an ensemble of thin, laminar,

locally one-dimensional flames, called flamelets, embedded within the turbulent flow field. The flamelet assumption states that most variables, like species concentrations and temperature, can be assumed to be dependent on a small number of control variables which are relevant for the flamelets which the turbulent flame is thought to be composed of. This will result in a simplification of the combustion model which can be described with a lower number of independent variables: mixture fraction, Z, which defines the mass fraction of methane (in our case) in the unburnt gas mixture, or the progress variable, PV, showing the evolution state of the combustion, are few of the independent variables describing the two types of combustion faced during this thesis project: premixed and non-premixed.

Implementation of FGM

[23] The implementation of the FGM method consists of three main steps:

1. Computing representative flamelets.
2. Building a look-up table.
3. Coupling the table with a flow solver.

These three steps will be explained in the following.

The first step consists of computing flamelets which are representative for the combustion system to which the FGM will be applied. It is obvious that when combustion takes place under (non-)premixed conditions in the application, the most representative flamelet is a (non-)premixed flamelet. The flamelets are computed by solving the flamelet equations:

[22] ***Premixed*** laminar flames are governed by the Navier–Stokes equations, the energy equation, and conservation equations for the species mass fractions, Y_i:

$$\frac{\partial}{\partial t}(\rho Y_i) + \nabla \cdot (\rho v Y_i) - \nabla \cdot (\frac{\lambda}{c_p Le_i} \nabla Y_i) = \dot{w_i}^+ - \dot{w_i}^- \tag{2}$$

with ρ the mass density, v the flow velocity, λ the thermal conductivity, c_p the specific heat and i the i-th species. The diffusive transport of the species

is described by a Fick-like approximation, where the Lewis numbers (defined as $Le_i = \frac{\lambda}{\rho D_i c_p}$, with D_i the diffusion coefficient of species i-th) are assumed constant and non-unity. The chemical source term has been divided in a production part $\dot{w_i}^+$ and a consumption part $\dot{w_i}^-$. Because of the assumption of steady state the left hand side of the equation can be neglected leaving a balance between chemical production and consumption. A better approximation of the mixture composition in the convection-diffusion-reaction region of a premixed flame can be found if the most important transport processes are also taken into account. Consider a curve $x(s)$ through a premixed flame, locally perpendicular to isosurfaces of a certain species mass fraction Y_i and parametrized by the arch length s. The evolution of each species mass fraction Y_i along this curve may be described approximately by a 1-D equation equivalent of the previous one:

$$m\frac{\partial Y_i}{\partial s} - \frac{\partial}{\partial s}(\frac{\lambda}{c_p Le_i}\frac{\partial Y_i}{\partial s}) = \dot{w_i}^+ - \dot{w_i}^- + P_i(s,t) \tag{3}$$

with m taken to be a constant mass flow rate. Transient and multi-dimensional effect, e.g. flame stretch and curvature, are gathered in the perturbation term $P_i(s,t)$. The curve is perpendicular to the isosurfaces of the i-th species mass fraction then the diffusive transport part is represented by the second term in the left-hand side. In most cases in premixed laminar flames P_i is smaller than other terms. The perturbation can be neglected if the curvature of the flame front is much larger than the flame thickness δ, the transient time scales are longer than the chemical time scales and if the Karlovitz number is small. The remaining equation together with a similar 1-D equation for the enthalpy constitute a set of equations called FLAMELET EQUATIONS which can be treated as 1-D STEADY LAMINAR UNSTRETCHED PREMIXED FLAME. Its solution form a 1-D curve in space parametrized by s. This curve can be considered as a 1-D MANIFOLD. This method can be extended to a multi-dimensional manifold of d dimensions generated by a $(d-1)D$ starting "plane". The strength of FGM reduction technique is that the number of independent control variables can be increased straightforward for increased accuracy. If variations in a conserved variable are expected to be important in the application, then this variable should be added as an extra controlling variable: the more variables we use to create the manifold, the more accurate the combustion process model and the higher computational cost affects the simulation.

For ***non-premixed*** combustion, in order to reduce the complexity of the problem and thus the number of equations to be solved a one-dimensional diffusion flame structure for chemistry tabulation is investigated by means of IGNITING COUNTERFLOW DIFFUSION FLAMELETS. It is a diffusion problem because when n-dodecane is injected into the combustion chamber it is non-premixed unlike the methane/air mixture which is premixed. Flamelets for non-premixed combustion can be generated using a geometry consisting of opposed, axisymmetric fuel and oxidizer jets, where they form a reaction zone close to the stagnation plane. The set of one-dimensional equations describing unsteady counterflow diffusion flames [2], [20] reads

$$\frac{\partial \rho}{\partial t} + \frac{\partial \rho u}{\partial x} = -\rho K \tag{4}$$

$$\frac{\partial \rho Y_k}{\partial t} + \frac{\partial \rho u Y_k}{\partial x} = \frac{\partial}{\partial x}\left(\rho D \frac{\partial Y_k}{\partial x}\right) + \dot{w}_k - \rho K Y_k \tag{5}$$

$$\frac{\partial \rho h}{\partial t} + \frac{\partial \rho u h}{\partial x} = \frac{\partial}{\partial x}\left(\frac{\lambda}{c_p}\frac{\partial h}{\partial x}\right) - \rho K h \tag{6}$$

and hence the diffusion coefficient is $D = \frac{\lambda}{\rho c_p}$. The local flame stretch rate K follows from the transport equation

$$\frac{\partial \rho K}{\partial t} + \frac{\partial \rho u K}{\partial x} = \frac{\partial}{\partial x}\left(\mu \frac{\partial K}{\partial x}\right) + \rho_{ox} a^2 - 2\rho K^2 \tag{7}$$

Here ρ_{ox} and a denote the density and prescribed strain rate in the oxidiser stream.

The LES approach (the one we chose to compute the CFD results) accounts for the eddies that are not resolved by means of the so called "closure-problem" for the unknown correlations that occur in the PDEs describing turbulent reacting flows. To model turbulence, the $k - \epsilon$ model which solves equations for the turbulent kinetic energy k and the turbulent kinetic energy dissipation rate ϵ is used. The turbulence-chemistry interaction is considered for progress variable and mixture fraction by means of a ***presumed $\beta -$ PDF*** model (Probability Density Function): thermochemical quantities ϕ, such as temperature, species mass fractions, fluid properties, and the progress

variable source term, are given by

$$\phi = F(Z, c) \tag{8}$$

where F is the functional relation governed by the flamelet equations.

Turbulence influences the combustion chemistry by distorting the flame. Turbulence-chemistry interaction is described in a stochastic way instead of a deterministic way, so this stochastic description of variables is appropriate just using the PDF filter, considering the probability of occurrence for several turbulent states instead of only one fixed state that can occur. The PDF can be thought of as the fraction of time that the fluid spends in a turbulent state. Hence all the thermochemical quantities are then calculated according to

$$\tilde{\phi} = \int_0^1 \int_0^1 \phi(Z, c)\tilde{P}(Z, c)dZdc \tag{9}$$

in which

$$\tilde{P}(Z, c) = \tilde{P}(Z)\tilde{P}(c) \tag{10}$$

This convolution operation generates an increase of two dimensions in the manifold, which reaches the number of four dimensions. The four degrees of freedom for the manifold are: progress variable, mixture fraction and their variances [13]:

$$\tilde{Z} \tag{11}$$

$$\tilde{Z''^2} \quad \in [0, \tilde{Z}(1 - \tilde{Z})] \tag{12}$$

$$\tilde{c} \tag{13}$$

$$\tilde{c''^2} \quad \in [0, \tilde{c}(1 - \tilde{c})] \tag{14}$$

While in the premixed case the above mentioned conserved scalar mixture fraction, Z, is assumed to be constant in case the blend is homogeneous, in the non-premixed case it tells in a way about the concentration of the n-dodecane along the axial direction of the counterflow diffusion flamelet (see Figure 10) and plays an essential role because helps locate the diffusive flame as together with the mixture fraction variance $\tilde{Z''}^2$, the probability density function can be calculated which in turn delivers the probability of finding the flame surface anywhere in the flow field. The progress variable variance $\tilde{c''}^2$ helps locate the flame front in premixed combustion.

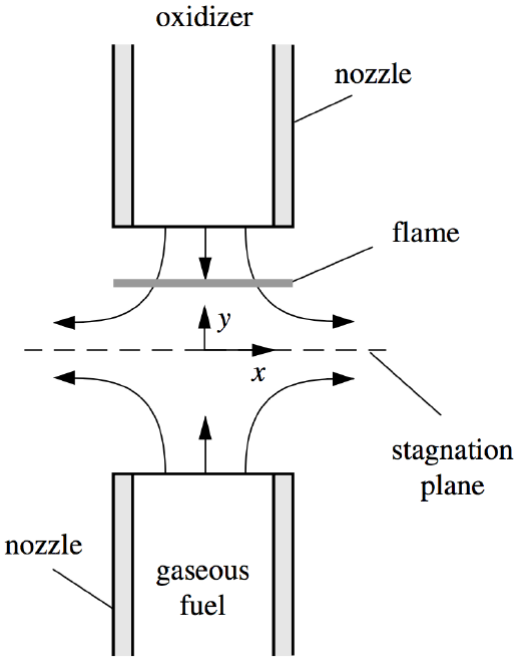

Figure 10: Schematic illustration of an experimental configuration for counterflow diffusion flames [11].

According to Bilger's equation [5] the mixture fraction is defined as:

$$Z = \frac{0.5\frac{Y_H - Y_{H,2}}{M_H} + 2.0\frac{Y_C - Y_{C,2}}{M_C} - \frac{Y_O - Y_{O,2}}{M_O}}{0.5\frac{Y_{H,1} - Y_{H,2}}{M_H} + 2.0\frac{Y_{C,1} - Y_{C,2}}{M_C} - \frac{Y_{O,1} - Y_{O,2}}{M_O}} \tag{15}$$

Y and M are the mass fraction and molecular mass, respectively. Subscripts C, H, O refer to the carbon, hydrogen and oxygen elements and

subscripts 1, 2 to the pure fuel and pure oxidizer concentrations, respectively. Thus $Z = 0$ is on the axial position for which only oxidizer is found and $Z = 1$ for fuel only. In the FGM approach, the progress of chemical reactions is captured by the control variable apart from time. This variable (c or PV) is chosen such that it describes the progress of the combustion process from the unburned mixture till chemical equilibrium. The only prerequisite is that the progress variable is monotonic in time and if normalized then it ranges between 0 (fresh mixture) and 1 (chemical equilibrium). The definition of c is usually chosen as a linear combination of species mass fractions

$$c = \sum_{i=1}^{N} \alpha_i Y_i \tag{16}$$

with α_i the weight factor of species i.

In order to solve the complex reaction mechanisms involved in combustion chemistry and to create the database of flamelets it is essential to apply a chemical kinetic model. We used ***CHEM1D*** model to solve partial differential equations (PDEs) for the laminar combustion combined to the ***Polimi*** one. Polimi is a mechanism which was developed at the Polytechnic University of Milan by Ranzi et al. [14], [15]. It performs quite well the combustion reactions with a rather low number of species and a relatively low computational time. The flamelet solutions are calculated by ***Clio*** which is a flamelet solver.

Once the 4-D manifolds are generated for both types of combustion by solving the flamelet equations, which are now parametrized by means of the four main scalars (means and variances of mixture fraction and progress variable), they can be used to retrieve the thermochemical quantities stored in them by coupling a specific thermochemical condition of the blend to a combination of the four independent variables.

The tabulated data includes for instance the progress variable source term, *csource*, which determines the ignition delay in the combustion spray, and species mass fractions to represent the composition of the mixture.

In the figures below is a list of all the scalars retrieved for our simulation.

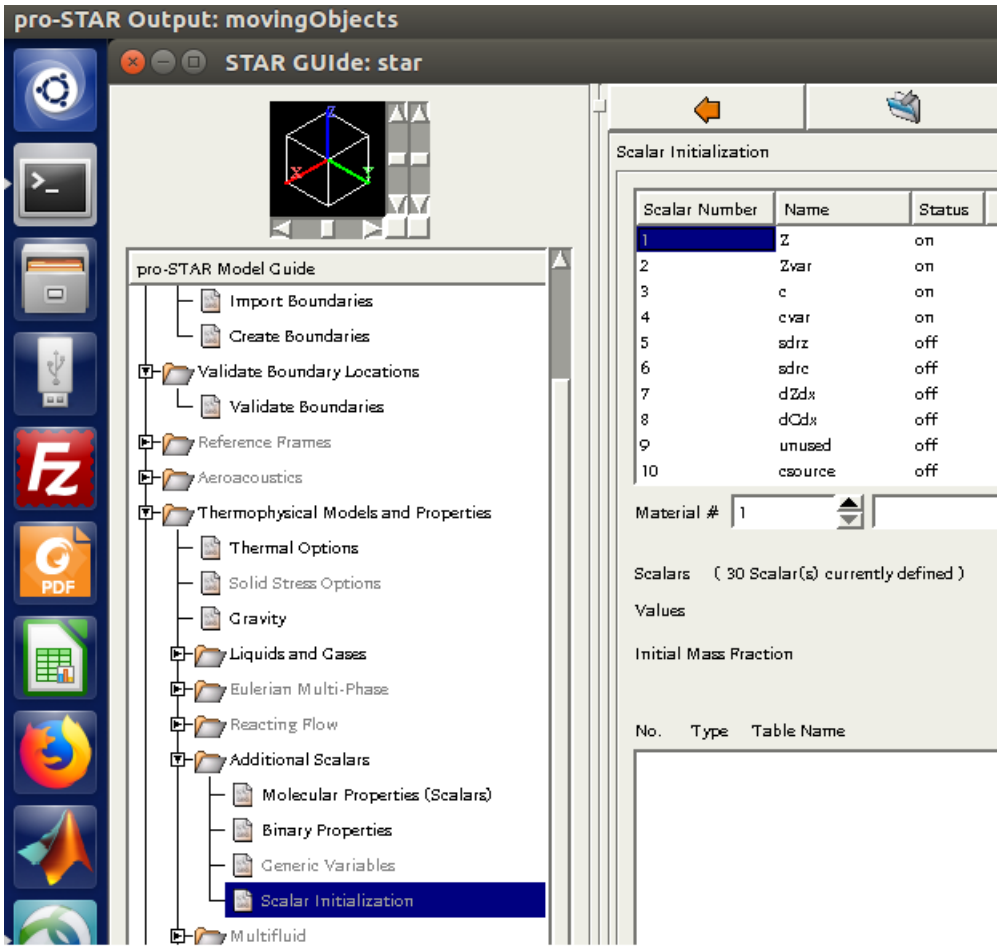

Figure 11: Scalars initialization in Pro-Star (1).

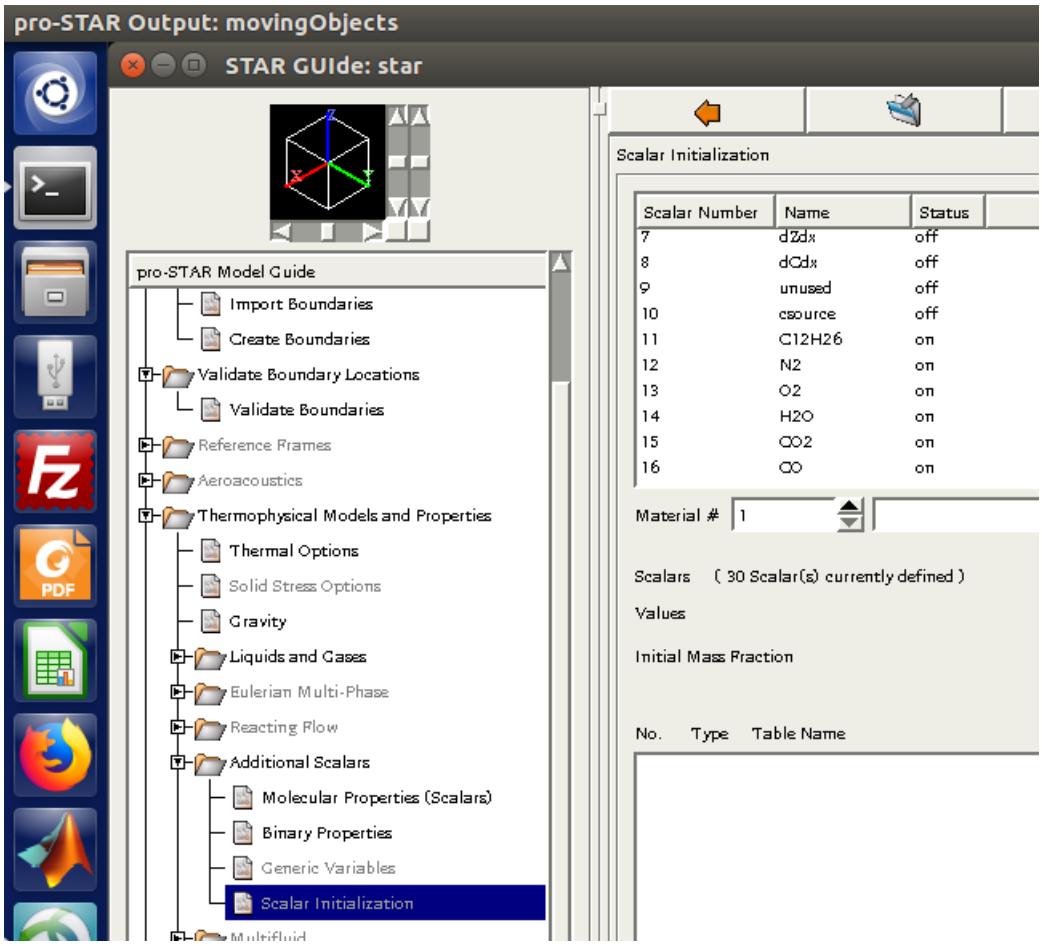

Figure 12: Scalars initialization in Pro-Star (2).

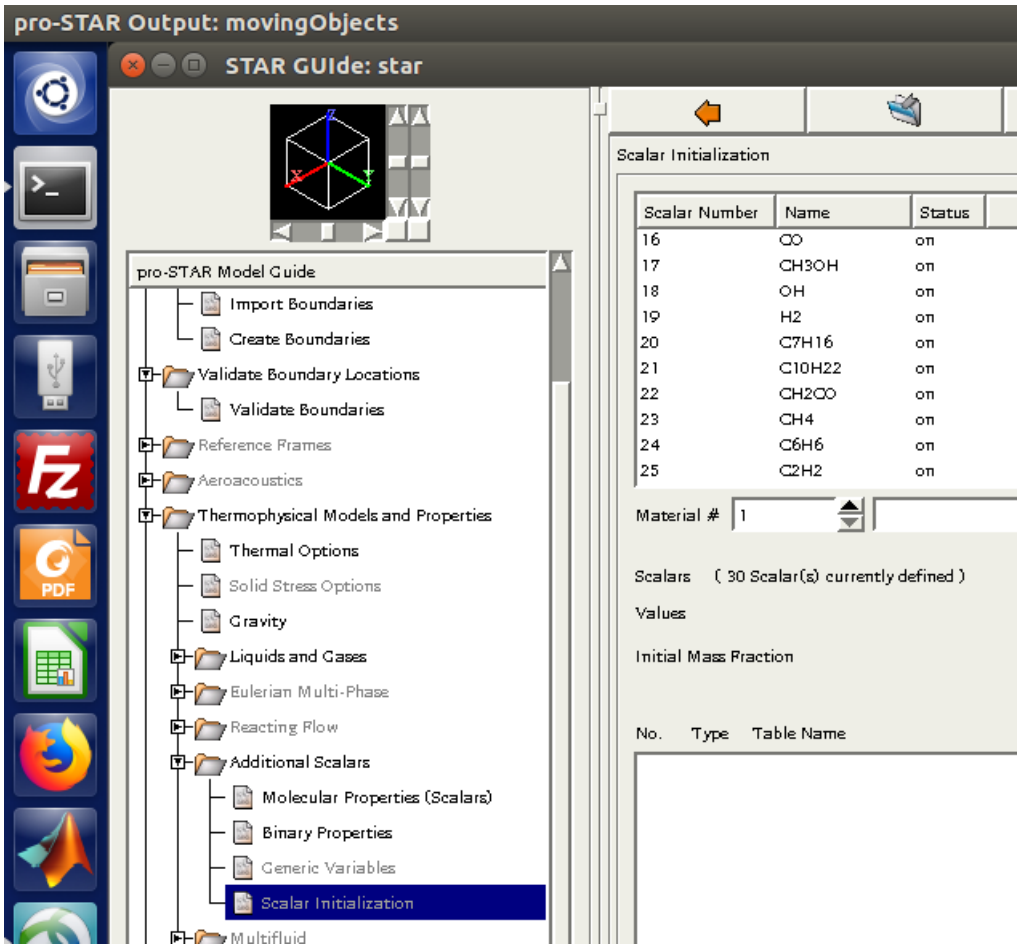

Figure 13: Scalars initialization in Pro-Star (3).

Computational set-up

Through this section we discuss the pre-processing steps and CFD tools settings, providing the reader with the basic knowledge of the way we ran the dual fuel marine propulsion system simulations keeping in mind that the whole engine cycle is divided in non-reactive and reactive case.

AS for the non-reactive phase, LES computations are started just before the EVO, at $-260\,°CAaTDC$ of combustion. Though we have already made mention of the initial and boundary conditions in table 2 in the introductory chapter, here we get insights over the logical steps to aim to a successful simulation rather than looking at the parameters values initialized to lunch the simulation.

The Winterthur Gas & Diesel AG company provided us with the geometrical mesh and all the operating condition parameters they got from the experimental analysis at bench test. So we checked the correctness of the geometrical features and of the computational grid, assessing for the latest if in the domain we were working on with LES method, mesh size was respecting the inertial turbulent zone so that grid cells are smaller than large scale phenomena and bigger than smaller scales that would be filtered by the LES model itself.

The mesh grid consists in 1.5 million of cells of type hexahedral on which the turbulent model ($k-\epsilon/High\ Reynolds\ Number$), the thermal model ($Static\ Enthalpy\ Conservation$) and the FGM combustion equations were solved with a time step ranging between 0.0025 and 0.01 $°CA$ which led to a computational runtime of 60 hours on 24 cores for a whole reactive ICE cycle.

As first step we fixed the simulation settings in *es-ice* CFD tool starting by the non-reactive phase and matching the computed pressure trace with the average IMEP chosen as representative of the in-cylinder pressure trend: we did that just fixing with criteria the boundary conditions so that the continuity equation was respected, as the amount of gas inside the cylinder before the EVO must be the same after the methane injections.

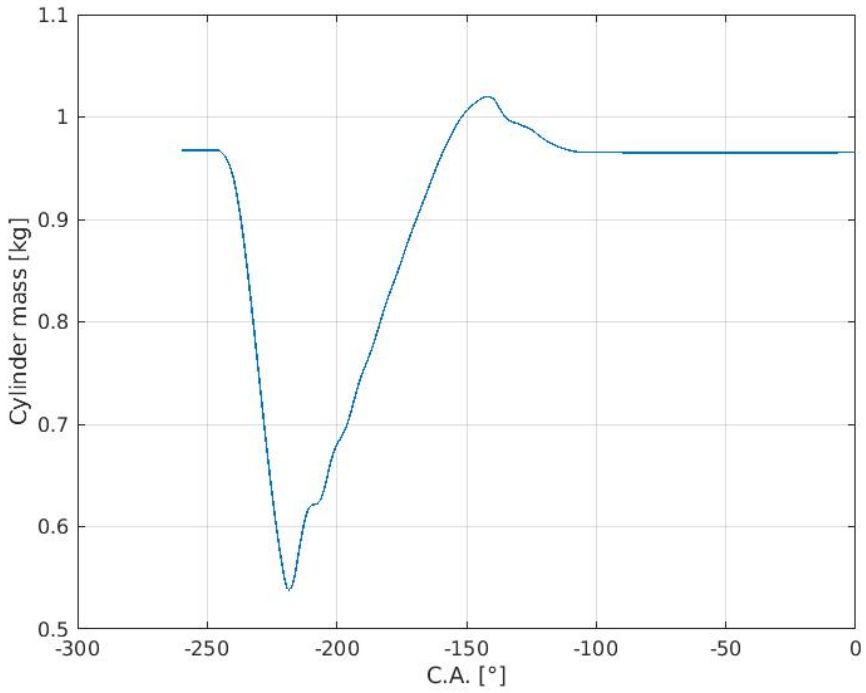

Figure 14: In-cylinder mass trend for the non-reactive phase.

The reliability of this first step can be assessed by noticing the perfect overlap of the two pressure traces, like showed in the figure below.

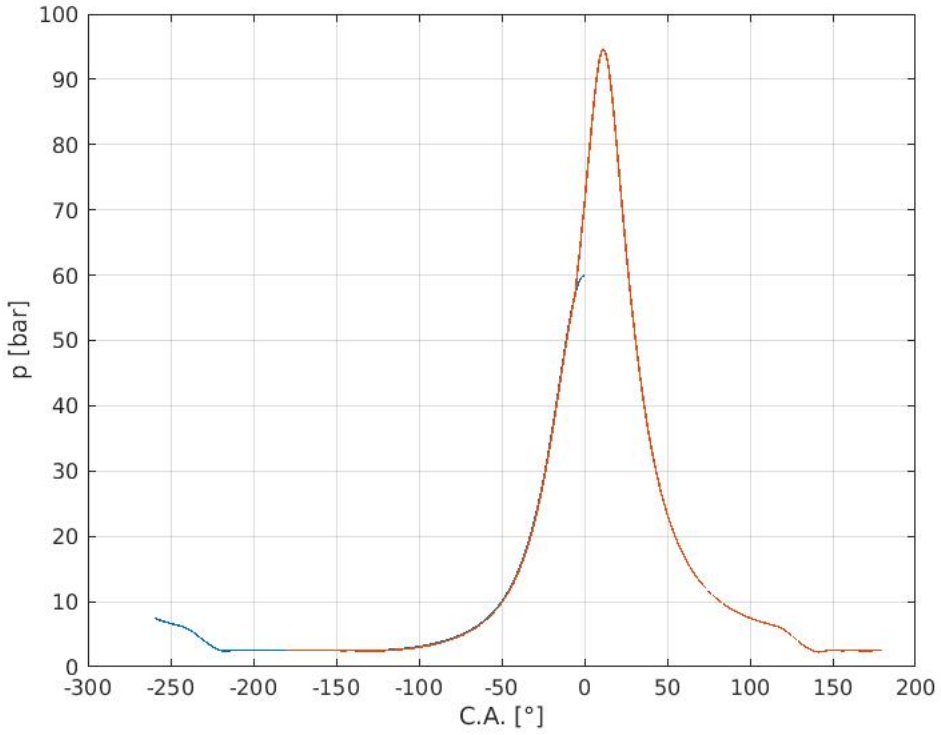

Figure 15: Computed (blue line) and experimental (red line) IMEP.

We moved on including the look-up 4-D FGM manifolds to recall the flamelets solutions so that we were able to solve the chemical reactions. After running the simulations we analysed the results stored in *star.spd* and *star.spg* files processing them in Matlab and then obtaining the most interesting and remarkable plots to draw proper conclusions over the compared combustion models: the standard PVM (Progress Variable Model) implemented by default in *Prostar* and the FGM (Flamelet Generated Manifold) model. The latter comparison is given in the next chapters about results and conclusions.

Upon combining the reactive case with the non-reactive one we parametrized the combustion process by means of three control variables to determine their different influences over the combustion reaction. The purpose of this is to analyse the aspects which need to be improved in the next future to get the most efficient combustion process starting from this dual fuel marine engine

design.

The control parameters took into account are:

- *Progress Variable variance*, defined as $PVvar = PV*(1-PV)$. Whether $PV = 0$ or $PV = 1$ the cell of the grid is composed only of reactants or products so there are no reactions and the reaction rate is obviously null.
- $PVsource$ (or *Csource*) ignition term, which includes two components: the source term for the premixed case which needs to be ignited by the source term of the non-premixed combustion (since we need the Diesel ignition to start the methane combustion). In such a way we took as control variable a parameter in the second term which affects the Diesel ID (Ignition Delay).
- *Methane mixture fraction*, Z, for both homogeneous blend case and for stratified charge.

Results and discussion

Control parameter: Progress Variable variance

In the first case the $PVvar$ is changing while the $Csource$ equals to 0.3 and Z is kept constant ($\lambda = 2.5$, homogeneous blend case).

In the multi-line plot below we can assess the effect of the $PVvar$ on the in-cylinder pressure averaged over both the main chamber and the two pre-chambers: its increase leads to a reduction of the pressure peaks (remember the formula for the $PVvar$) due to a less chemically-reactive blend.

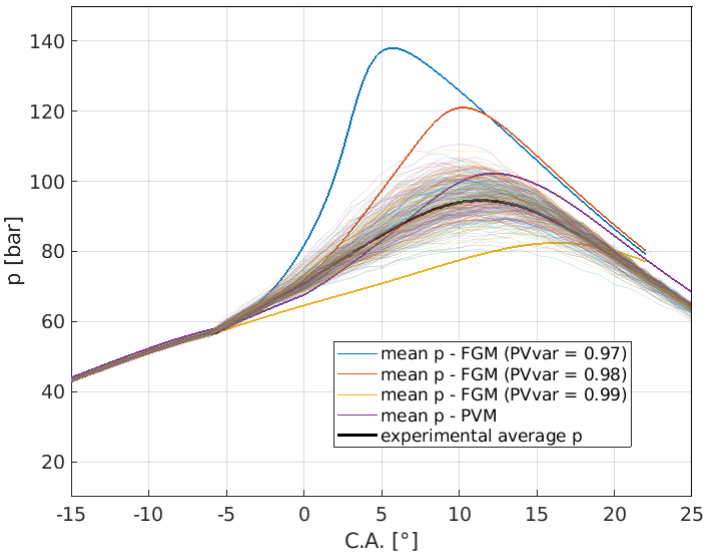

Figure 16: In-cylinder IMEP and cyclic variation.

Just looking at the curves with $PVvar = 0.99$ and 0.98 we can find out that the matching value (the needed one for overlapping the computed

pressure trace with the experimental IMEP) should be around 0.985: that is actually the *PVvar* value considered in the next cases.

The next multi-line plot shows that the growth of *PVvar* pushes down the pressure peaks inside the pre-chambers. As both the pre-chambers got the same identical results, we decided to put here just the results' trends for one of the two pre-chambers, which conventionally called "positive pre-chamber" to distinguish it from the "negative pre-chamber". It is obvious that whenever the reactivity of the combustion drops, the maximum peak pressure inside the pre-chambers falls down and in turn the average pressure in the whole cylinder follows the same trend.

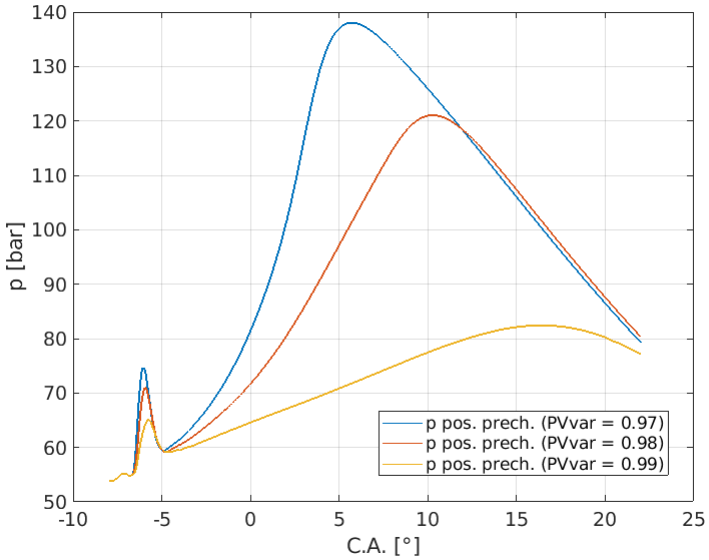

Figure 17: Positive pre-chamber IMEP.

Still if the premixed combustion rate reduces the normalized PV trend slows down.

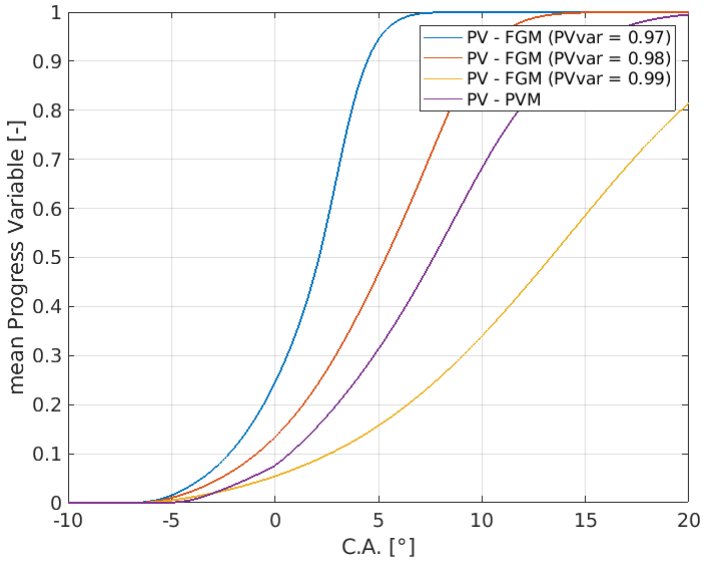

Figure 18: In-cylinder Progress Variable.

The example case with $PVvar = 0.97$ it is noteworthy to point out the delay (of almost 5 °CA) between the PV in the pre-chambers and in the Region1/main chamber (the Region1 includes both the other two): since this is an averaged value and cause of the big difference between pre-chambers and main chamber volume, the PV trends in the Region1 and in the main chamber overlap.

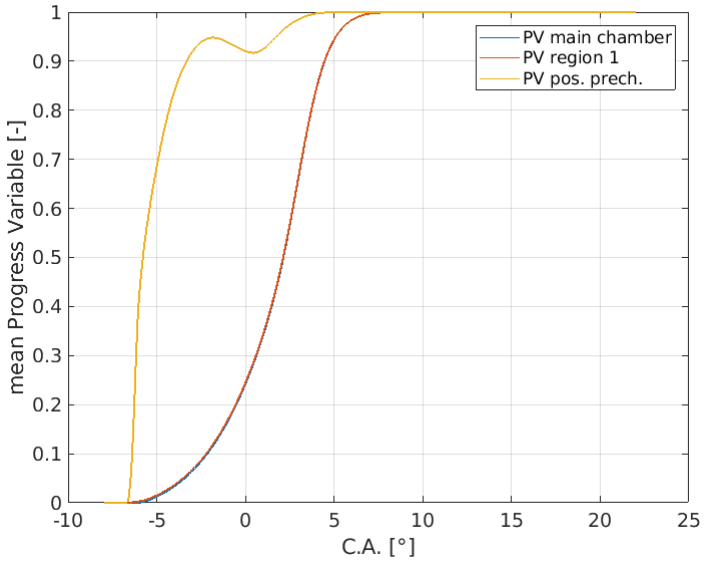

Figure 19: Premixed combustion process delay between three different cylinder regions.

In line with what we said previously the increasing $PVvar$ reduces the pre-chamber temperature and therefore the pressure inside the pre-chambers, leading to a reduction of the jets velocity magnitude at the pre-chambers' outlets.

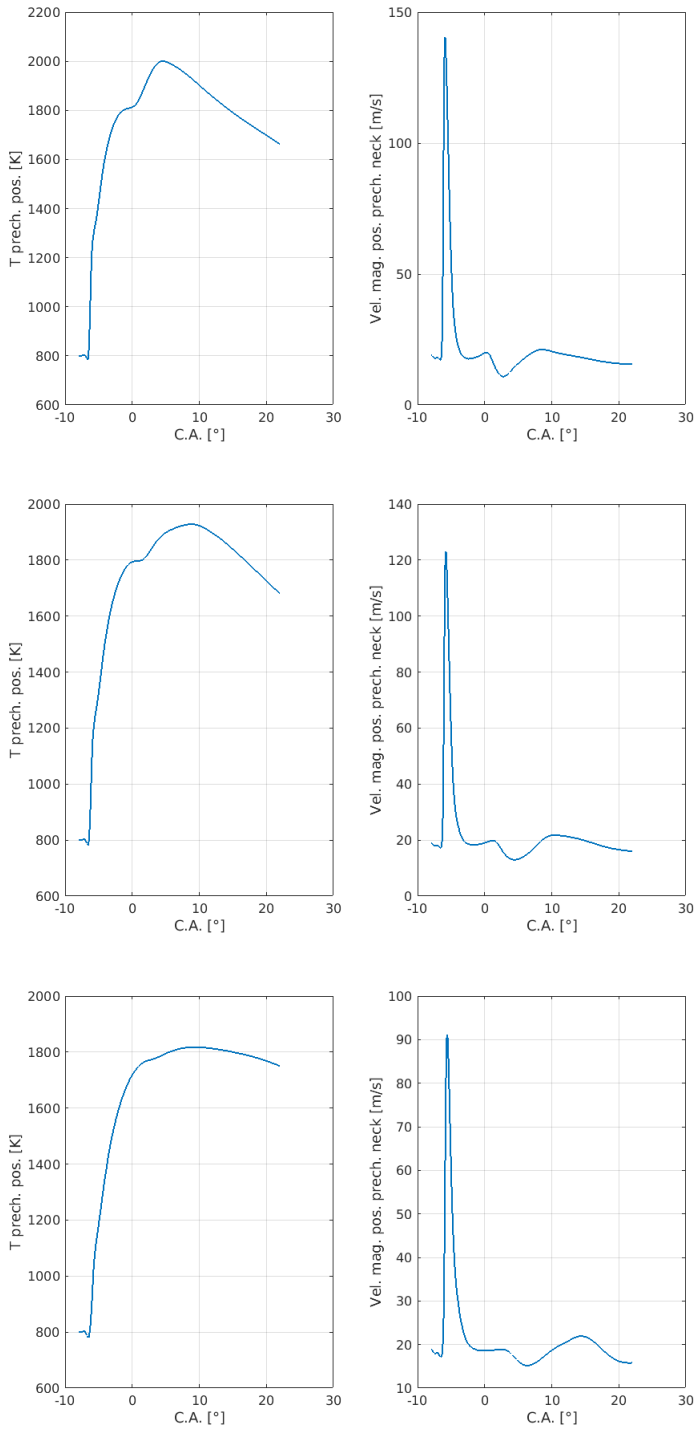

Figure 20: From top to bottom: *PVvar=0.97*, *PVvar=0.98*, *PVvar=0.99*.

Below is represented the qualitative analysis of the evolution of the two jets coming out the pre-chambers for the three $PVvar$ cases between -6 and $+6\,°CAaTDC$ of combustion with interval steps of $4\,°CA$.

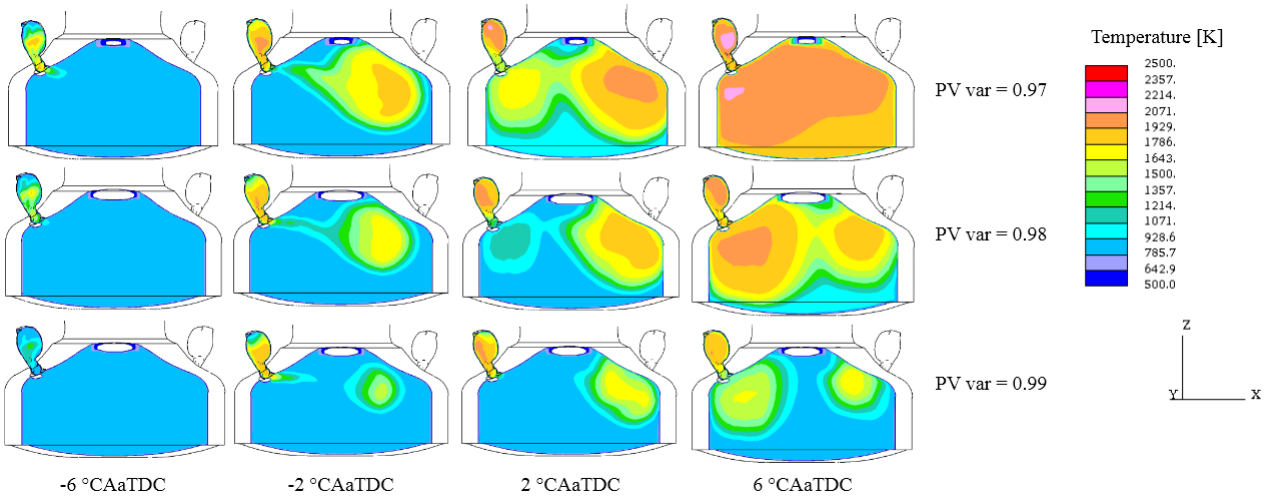

Figure 21: Jets evolution: temperature inside the cylinder during the premixed combustion process.

Control parameter: Csource ignition term

Let us move on to the second case with $PVvar = 0.985$, Z homogeneous and *Csource* ignition variable (we are going to assess its influence): whenever it increases the ID (Ignition Delay) goes down. The effect of the Diesel ID is more reduced than the premixed combustion reaction rate effect and consequently all the three pressure traces are so close each other that there is almost an overlap and all of them are closer to both the PVM trend and the experimental average pressure. Because of the reduction in the ID, the pre-chambers pressures are anticipated but their peaks values remain almost the same.

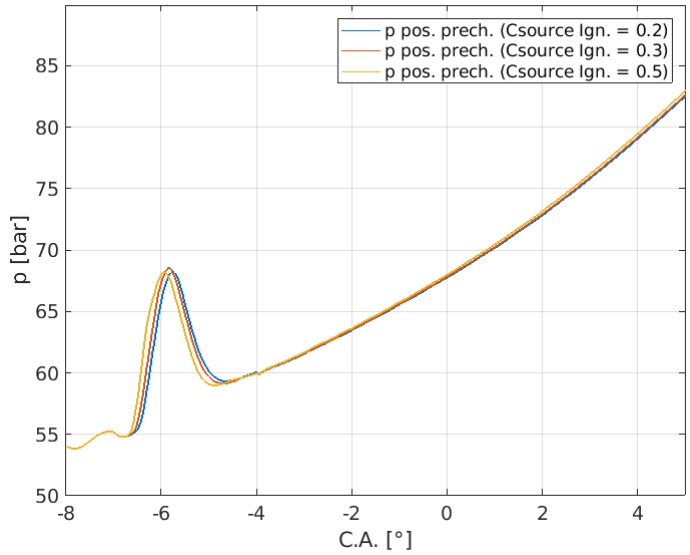

Figure 22: Positive pre-chamber IMEP.

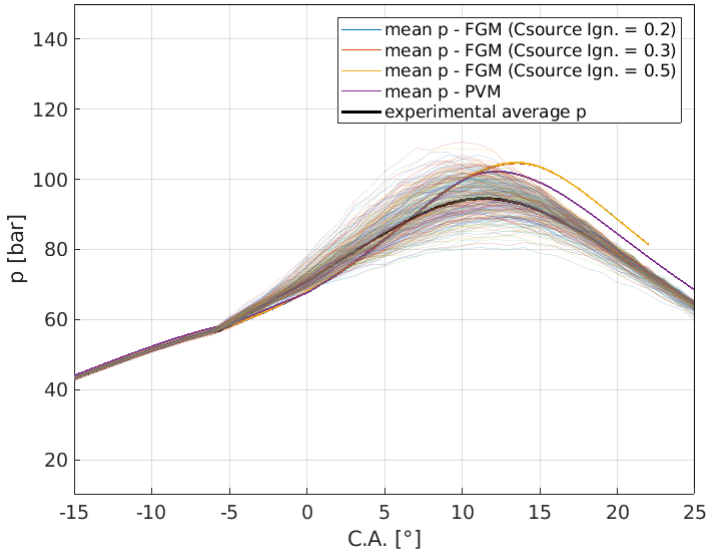

Figure 23: In-cylinder IMEP and cyclic variation.

Obviously, the PV curve inside the pre-chambers is anticipated while the *Csource* ignition term increases.

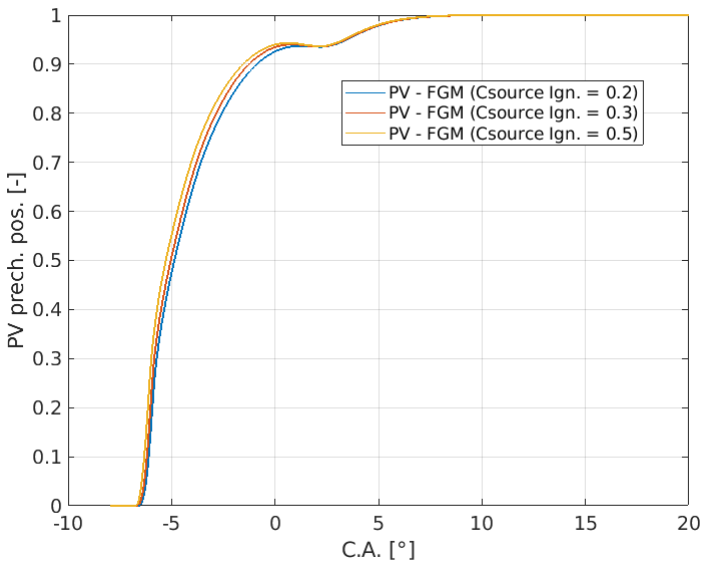

Figure 24: Premixed combustion delay due to the *Csource* term.

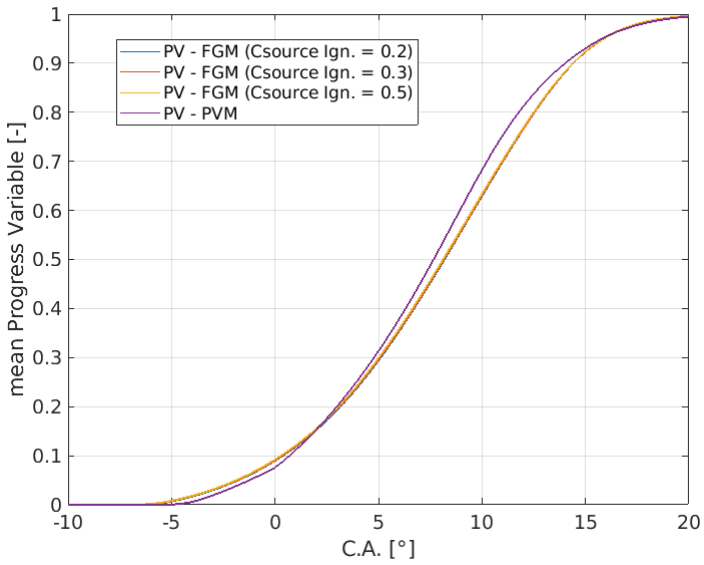

Figure 25: In-cylinder Progress Variable.

Control parameter: methane mixture fraction

In the last case we assess the influence of a more realistic blend composition, namely a stratified charge ranging between $\lambda = 3$ and $\lambda = 2.5$, over the combustion process. The pressure curves with a stratified blend get lower pressure peaks compared to the homogeneous mixture since in this case in the middle region of the cylinder the methane concentration is leaner than before, and the flame front propagation is slowed down.

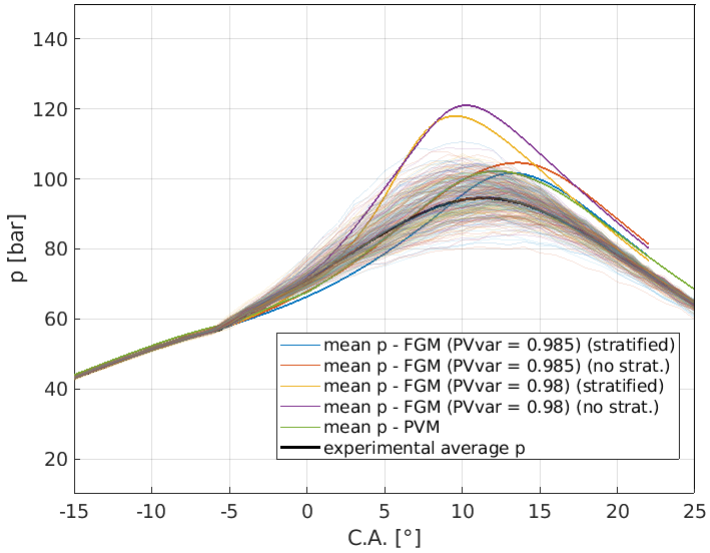

Figure 26: In-cylinder IMEP and cyclic variation.

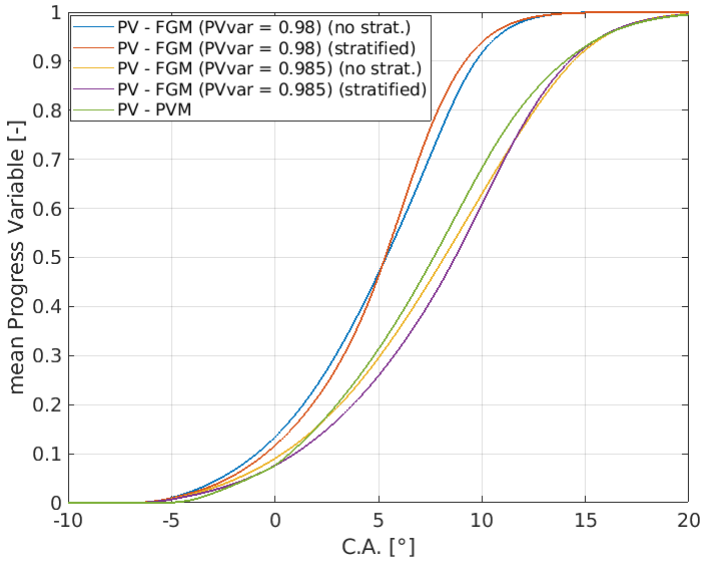

Figure 27: In-cylinder Progress Variable.

Conclusion and outlook

To sum up the predictive *Flamelet Generated Manifold* model underlines an higher sensitivity to the $PVvar$ rather than to other control parameters and because of the high cyclic variation, the case with $PVvar = 0.985$, $Csource = 0.3$ and stratified charge, despite the experimental average pressure trend is not completely matching, can be considered acceptable for our purposes along with the Winterthur Gas & Diesel AG aims. The pre-chambers strategy could be further investigated in the future by changing the Diesel injectors, modifying the geometry of the pre-chambers' outlets and therefore trying to get higher performance and efficiency. Still the PVM and FGM model are valid combustion models and provided us with good results for the simulations, in fact the thermodynamic quantities are close enough to the expected one.

In view of possible future outlooks the pre-chamber strategy could be further investigated to improve the premixed combustion process and one could study different operating conditions to get an overall view of the engine efficiency and its weaknesses.

Bibliography

[1] I. Ahmed, G. Ghiasi, A. G. S. Raj, N. Swaminathan, J. Koch, K. Steurs, and Y. M. Wright. Spark ignition engine simulation using a flamelet based combustion model. Technical report, SAE Technical Paper, 2015.

[2] G. Dixon-Lewis, T. David, P. Gaskell, S. Fukutani, H. Jinno, J. Miller, R. Kee, M. Smooke, N. Peters, E. Effelsberg, et al. Calculation of the structure and extinction limit of a methane-air counterflow diffusion flame in the forward stagnation region of a porous cylinder. In *Symposium (International) on Combustion*, volume 20, pages 1893–1904. Elsevier, 1985.

[3] A. Donini, R. Bastiaans, J. van Oijen, and L. de Goey. A 5-d implementation of fgm for the large eddy simulation of a stratified swirled flame with heat loss in a gas turbine combustor. *Flow, Turbulence and Combustion*, 98(3):887–922, 2017.

[4] T. Echekki and E. Mastorakos. *Turbulent combustion modeling: Advances, new trends and perspectives*, volume 95. Springer Science & Business Media, 2010.

[5] U. Egüz, S. Ayyapureddi, C. Bekdemir, B. Somers, and P. de Goey. Modeling fuel spray auto-ignition using the fgm approach: effect of tabulation method. Technical report, SAE Technical Paper, 2012.

[6] P. F. Flynn, R. P. Durrett, G. L. Hunter, A. O. zur Loye, O. C. Akinyemi, J. E. Dec, and C. K. Westbrook. Diesel combustion: an integrated view combining laser diagnostics, chemical kinetics, and empirical validation. Technical report, SAE Technical Paper, 1999.

[7] R. S. Laramee, D. Weiskopf, J. Schneider, and H. Hauser. Investigating swirl and tumble flow with a comparison of visualization techniques. In *Visualization, 2004. IEEE*, pages 51–58. IEEE, 2004.

[8] M. G. Masouleh, A. Wehrfritz, O. Kaario, H. Kahila, and V. Vuorinen. Comparative study on chemical kinetic schemes for dual-fuel combustion of n-dodecane/methane blends. *Fuel*, 191:62–76, 2017.

[9] J. v. Oijen and L. d. Goey. Modelling of premixed laminar flames using flamelet-generated manifolds. *Combustion Science and Technology*, 161 (1):113–137, 2000.

[10] R. Papagiannakis and D. Hountalas. Combustion and exhaust emission characteristics of a dual fuel compression ignition engine operated with pilot diesel fuel and natural gas. *Energy conversion and management*, 45 (18-19):2971–2987, 2004.

[11] N. Peters. *Turbulent combustion*. Cambridge university press, 2000.

[12] H. Pitsch. A consistent level set formulation for large-eddy simulation of premixed turbulent combustion. *Combustion and Flame*, 143(4):587–598, 2005.

[13] W. Ramaekers, de Goey (LPH), van Oijen (JA), B. Albrecht, and R. Eggels. *The application of flamelet generated manifolds in modelling of turbulent partially-premixed flames*. Technische Universiteit Eindhoven, 2005.

[14] E. Ranzi, A. Frassoldati, R. Grana, A. Cuoci, T. Faravelli, A. Kelley, and C. Law. Hierarchical and comparative kinetic modeling of laminar flame speeds of hydrocarbon and oxygenated fuels. *Progress in Energy and Combustion Science*, 38(4):468–501, 2012.

[15] E. Ranzi, A. Frassoldati, A. Stagni, M. Pelucchi, A. Cuoci, and T. Faravelli. Reduced kinetic schemes of complex reaction systems: fossil and biomass-derived transportation fuels. *International Journal of Chemical Kinetics*, 46(9):512–542, 2014.

[16] S. Schlatter, B. Schneider, Y. Wright, and K. Boulouchos. Experimental study of ignition and combustion characteristics of a diesel pilot spray in a lean premixed methane/air charge using a rapid compression expansion machine. Technical report, SAE Technical Paper, 2012.

[17] S. Schlatter, B. Schneider, Y. M. Wright, and K. Boulouchos. Comparative study of ignition systems for lean burn gas engines in an optically accessible rapid compression expansion machine. Technical report, SAE Technical Paper, 2013.

[18] S. Schlatter, B. Schneider, Y. M. Wright, and K. Boulouchos. N-heptane micro pilot assisted methane combustion in a rapid compression expansion machine. *Fuel*, 179:339–352, 2016.

[19] S. Singh, S.-C. Kong, R. D. Reitz, S. R. Krishnan, and K. C. Midkiff. Modeling and experiments of dual-fuel engine combustion and emissions. Technical report, SAE Technical paper, 2004.

[20] G. Stahl and J. Warnatz. Numerical investigation of time-dependent properties and extinction of strained methane and propane-air flamelets. *Combustion and Flame*, 85(3-4):285–299, 1991.

[21] P. Trisjono, K. Kleinheinz, H. Pitsch, and S. Kang. Large eddy simulation of stratified and sheared flames of a premixed turbulent stratified flame burner using a flamelet model with heat loss. *Flow, turbulence and combustion*, 92(1-2):201–235, 2014.

[22] J. Van Oijen, F. Lammers, and L. De Goey. Modeling of complex premixed burner systems by using flamelet-generated manifolds. *Combustion and Flame*, 127(3):2124–2134, 2001.

[23] J. Van Oijen, A. Donini, R. Bastiaans, J. ten Thije Boonkkamp, and L. de Goey. State-of-the-art in premixed combustion modeling using flamelet generated manifolds. *Progress in Energy and Combustion Science*, 57:30–74, 2016.

[24] A. Wehrfritz, O. Kaario, V. Vuorinen, and B. Somers. Large eddy simulation of n-dodecane spray flames using flamelet generated manifolds. *Combustion and Flame*, 167:113–131, 2016.

[25] Y. Zhang, S.-C. Kong, and R. D. Reitz. Modeling and simulation of a dual fuel (diesel/natural gas) engine with multidimensional cfd. Technical report, SAE Technical Paper, 2003.